



**HAL**  
open science

# Critical Links Detection in Spatial-Temporal Airway Networks Using Complex Network Theories

Chunyao Ma, Qing Cai, Sameer Alam, Daniel Delahaye

► **To cite this version:**

Chunyao Ma, Qing Cai, Sameer Alam, Daniel Delahaye. Critical Links Detection in Spatial-Temporal Airway Networks Using Complex Network Theories. IEEE Access, 2022, 10.1109/ACCESS.2022.3152163 . hal-03581545

**HAL Id: hal-03581545**

**<https://enac.hal.science/hal-03581545>**

Submitted on 19 Feb 2022

**HAL** is a multi-disciplinary open access archive for the deposit and dissemination of scientific research documents, whether they are published or not. The documents may come from teaching and research institutions in France or abroad, or from public or private research centers.

L'archive ouverte pluridisciplinaire **HAL**, est destinée au dépôt et à la diffusion de documents scientifiques de niveau recherche, publiés ou non, émanant des établissements d'enseignement et de recherche français ou étrangers, des laboratoires publics ou privés.

Date of xxxx, date of current accepted version 2021.

Digital Object Identifier xxx.xxx

# Critical Links Detection in Spatial-Temporal Airway Networks Using Complex Network Theories

CHUNYAO MA<sup>1</sup>, QING CAI<sup>1</sup>, SAMEER ALAM<sup>1</sup>, DANIEL DELAHAYE<sup>2</sup>

<sup>1</sup>Air Traffic Management Research Institute, School of Mechanical and Aerospace Engineering, Nanyang Technological University, Singapore, 639798

<sup>2</sup>OPTIM Lab, Ecole Nationale de l'Aviation Civile, Toulouse, France

Corresponding authors: Qing Cai (e-mail: qcai@ntu.edu.sg), Sameer Alam (e-mail: sameeralam@ntu.edu.sg)

This research is supported by the National Research Foundation, Singapore, and the Civil Aviation Authority of Singapore, under the Aviation Transformation Programme. Any opinions, findings and conclusions or recommendations expressed in this material are those of the author(s) and do not reflect the views of National Research Foundation, Singapore and the Civil Aviation Authority of Singapore.

## ABSTRACT

In an airway network, some critical links exist that are vital for the structural integrity and performance of the network. The detection of such links may assist with improving the imbalance between the limited airspace capacity and the ever-increasing traffic demand, which elicit flight delays, significant economic losses, etc. However, it is challenging to identify such links as they evolve (both in space and time) with changing traffic flow dynamics. This paper proposes a complex network approach for spatial-temporal critical links detection in a given airway network. First, flight track data is employed to characterize the airway network as weighted spatial-temporal networks. Then edge centrality and network percolation metrics are adopted to detect the critical links in each snapshot of the spatial-temporal networks. Afterward, the critical links detected by the two metrics are spatially overlapped to determine the final critical links over time. To examine the operational validity of the proposed method, we carry out a case study on the Southeast Asia airway network derived from one-month flight track data. Results demonstrate that the spatial distribution of the critical links varies over different traffic scenarios, and most of the identified critical links are found in the transition sectors with complex traffic situations. Four links, which are parts and at crosses of major trunk airways connecting to major navigation aids (VOR/DME) in the studied network, appear highly in all examined traffic scenarios. The unavailability of such links may lead to traffic flow disruptions. Observations by subject matter experts from air-traffic data visualizations demonstrate that the complex network-based methods can dynamically identify airway links that are operationally critical under time-evolving air-traffic scenarios. With good traffic flow prediction tools in the future, this method can be adopted to predict critical links in airway networks to better assist controllers in real-time air traffic management.

**INDEX TERMS** Air transportation, airway network, spatial-temporal network, critical link detection, network centrality, percolation theory

## I. INTRODUCTION

Although the air traffic demand during the outbreak of the COVID-19 pandemic almost came to a standstill, the traffic demand is now on its way to ramping up across nations as many traveling restrictions are lifted [1]. To accommodate the projected air traffic demand, air transport system needs to continuously evolve both in terms of infrastructure and operationally [2]. Currently, the biggest challenge confronted by air navigation service providers (ANSPs) is the capacity-demand dilemma, as known as the imbalance

between airspace capacity and traffic demand [3], [4], which is the major source for en-route congestion that elicits not only traffic delays, but also environmental impact [5], [6]. Note that the en-route phase of aircraft is based on flight plans which typically follow airway networks with intermediate waypoints (nodes) forming the links in the network. An airway network constitutes the virtual highway in the sky on which the air traffic operates. Therefore, it is very promising to manage congestion by improving air traffic flow on airway networks [7], [8].

In the literature, some researchers aim to optimize the network traffic flow to mitigate traffic congestion. For example, in [9], a network-based dynamic air traffic flow model for en-route airspace traffic flow optimization was proposed to maintain the balance between demand and capacity. In [10], a collaborative flight route-planning method was demonstrated to reduce en-route airspace congestion by amending flight plans to avoid congested sectors. The optimization of air traffic flow on airway networks adapts traffic flow to the airway network structure which is restricted by the structure of the airway network. Therefore, some researchers propose to mitigate congestion by optimizing the designs of airway networks [7]. In [11], a multi-objective optimization algorithm was introduced to optimize the crossing waypoint locations of Air Traffic Service (ATS) routes, with the objective being the maximization of the flight efficiency and airspace capacity. In [12], an airway network optimization model was developed to minimize the total operational cost with airspace restriction and air route network capacity being considered as the major constraints. In [13] the authors proposed to remove some links in the potentially over-designed airway networks based on the theory of Braess's Paradox. They discovered that the total flight duration on an airway network could be reduced by making minor changes to the airway network structure.

It should be pointed out that en-route congestion usually emerges locally in an airway network. The local congestion on some links can propagate to their vicinity [8], which then essentially impedes traffic flows in the airspace and exacerbates the traffic congestion. In the presence of limited airspace capacity and the saturated airway network, it is of great significance to identify such critical links in an airway network. Generally speaking, a critical link in a complex network is a link whose failure will significantly affect the network's performance in terms of structural integrity, functionality, etc [14]. When an airway network is of concern, we regard a critical link as the airway link (connecting two waypoints), which acts as a pivot link and whose failure may decrease the network's structural integrity concerning the given traffic scenario. Therefore, identification of such critical links in an airway network can assist air traffic managers with better traffic flow planning and decision making.

Critical links detection in complex networks is not new and has long been explored [15]–[17]. One of the most popular methods for critical links detection in complex networks is based on network centrality metrics [18]. A centrality metric provides a straightforward way of calculating how central a network's component is. The second widely adopted methods are based on network vulnerability analysis in the presence of link failures [19]. The underlying idea is that the critical links of a network should be the links whose failures will decrease its robustness in the face of perturbations [20], [21]. In recent years, many researchers have applied network theories to detect critical links in transportation networks by investigating the networks' performance such as the overall travel cost [22], the total demand losses [23], decreased

network capacity [24], etc.

Although various methods have been proposed for critical links detection in transportation networks, existing approaches mainly have three drawbacks. Firstly, methods like the one proposed in [25] are model-driven, neglecting the merits of real-world traffic data [26]. Secondly, many methods only consider a single metric such as network centrality metric [27], [28], traffic capacity [24], network robustness [29], [30], etc., to quantify the criticality of a network's links [16]. Multiple criteria should be taken into account for critical links detection for real application purposes to avoid uncertainty and unreliability [31]. Thirdly, as indicated in [32] that the majority of existing methods only deal with static networks, while real-world transportation networks are time evolving. Meanwhile, most if not all of the existing studies are urban traffic networks oriented [33], [34], rendering their direct applications to air traffic networks infeasible, given its four-dimensional nature. In this paper, we propose to detect critical links in airway networks using spatial-temporal network models. Note that the critical links in an airway network would evolve over time. Therefore, it is not reasonable to detect critical links in binary and static airway networks. In view of this, we first construct weighted spatial-temporal airway networks based on given flight track data. We then introduce edge betweenness centrality and network percolation theory to detect critical links in each snapshot of the temporal networks. Finally, comparisons among the detection results using the two metrics are made to determine the final critical links for the snapshot of the given traffic scenario. A case study is carried out on the Southeast Asia airway network which is derived from one-month flight track data for the calendar year 2018 to demonstrate the efficacy of the proposed method. The studied network covers the ATS routes in Singapore Flight Information Region (FIR) and transiting links between Singapore FIR and its neighbouring airspace. For the purpose of simplicity, we term this network as Southeast Asia Airway Network (SEAN) throughout the paper.

## II. RELATED BACKGROUNDS

### A. SPATIAL-TEMPORAL NETWORKS

A complex network is usually depicted by a graph that is composed of a set of node/vertices and links/edges. Mathematically, a graph  $G$  is denoted by  $G = \{V, E\}$  with  $V$  and  $E$  respectively being the sets of nodes and links. Usually, we use  $n = |V|$  and  $m = |E|$  to respectively denote the number of nodes and edges in  $G$ .

In reality, the nodes of complex networks like airway networks carry geographical coordination information. Such networks are generally called spatial networks. Note that some complex networks are time-evolving, i.e., their structures change over time. Such networks are generally called temporal networks. Mathematically, a temporal network  $G$  can be denoted by a network sequence, i.e.,  $G = \{G^{t_0}, \dots, G^{t_i}, \dots\}$  with  $G^{t_i}$  being the snapshot at time point  $t_i$  or for a certain time period. A complex network carrying

both spatial and temporal information is normally modelled as a spatial-temporal network.

### B. NETWORK CENTRALITY

For a given complex network, one may wish to know which nodes or edges are more important than others concerning the network structure. The network centrality metric provides an outlet for that purpose. In the literature, many centrality metrics are available [18], [35]. There are mainly two types of centrality metrics, viz., node centrality and edge centrality, while the latter is generally the extensions of the former ones.

In this study, we adopt edge centrality metrics as the purpose of this study is to detect critical links from a given airway network. Specifically, we adopt the betweenness centrality metric ( $C_E^B$ ), which has been tested to have a larger impact on a network's robustness [18]. For a given network  $G$ , the betweenness centrality for an edge  $e \in E$  is calculated as

$$C_E^B(e) = \frac{2}{n(n-1)} \sum_{i \neq j} \frac{p_{ij}(e)}{P_{ij}} \quad (1)$$

in which  $p_{ij}(e)$  is the number of shortest paths between nodes  $i$  and  $j$  running through edge  $e$ , and  $P_{ij}$  is the total number of shortest paths between nodes  $i$  and  $j$ .

### C. PERCOLATION THEORY

Complex networks, in reality, suffer from various perturbations. Consequently, the components of a network may break down, and potential risk is likely to happen. To better design the structure of a network to make it robust to perturbations, it is pertinent to analyse the dynamics of a complex network subject to perturbations. Percolation theory has proven as an effective instrument for analysing the capability of a complex network in the face of perturbations [36], [37].

Suppose that  $1 - p$  fraction of network components are disconnected to the rest of the focal network due to external/internal perturbations. The disconnection of those failed network components can fragment the focal network into pieces amongst which there exists the largest connected component (LCC) [38]. The LCC of a network is an essential indicator for capturing the network's capability in response to perturbations. When  $p = 0$ , the LCC of the network disappears, simulating the scenario that the focal network is entirely down due to perturbations. For  $p = 1$ , it corresponds to the situation that the network is not suffering from perturbations and the LCC keeps its original state. When  $p$  increases from 0 to 1, the size of the LCC changes with  $p$ . When  $p$  reaches a particular value, the size of the LCC shows a notable change, such as a sharp decline or becomes extremely small or even zero. Such a value of  $p$  is generally termed as the percolation threshold denoted by  $p_c$ .

## III. RESEARCH PROBLEM AND CONTRIBUTION

### A. PROBLEM DESCRIPTION

This paper aims to identify the critical links in a given airway network. In this paper, we define the critical links in an airway network from the network theory perspective. Specifically, we define the critical links as the airway links that meet the following two requirements:

- 1) the links act as the traffic pivots through which shortest paths frequently pass;
- 2) the links that act as the bridges whose failures will significantly decrease the network's structural integrity in the face of perturbations.

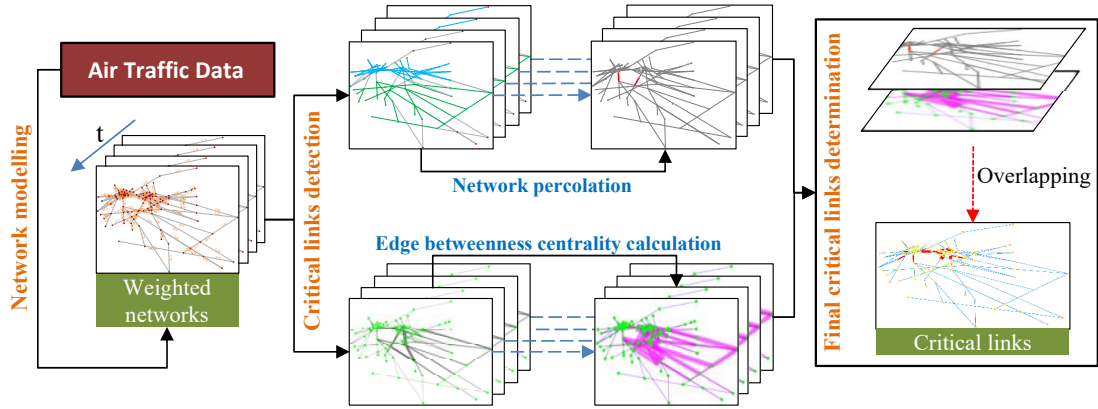
Note that for different traffic situations, the critical links may vary. Therefore, directly detecting critical links in a static and unweighted airway network is not of practical usage. Thus, in this paper, we propose to detect the critical links spatially and temporally for different traffic situations. Moreover, instead of using a single metric, two metrics in network theory, i.e., network centrality and percolation theory, are adopted and combined to identify the critical links in the spatial-temporal networks. Centrality is a widely applied metric for quantifying the importance of a network's components (nodes and links). Large centrality values can distinguish the pivots links through which shortest flight paths frequently pass, while the percolation theory is an effective method for measuring the structural integrity of a given network concerning network component failures.

Fig. 1 presents a graphical illustration of the studied research problem. In the network modelling step, for a given airway network, we process the flight track data to construct weighted spatial-temporal airway networks  $G = \{G^{t_0}, \dots, G^{t_i}, \dots\}$  with  $G^{t_i}$  being the weighted network snapshot built for a certain time period  $t_i$ . Then, we adopt centrality metric and network percolation theory to identify critical links from each network snapshot  $G^{t_i}$ . Finally, in the final critical links determination step, the critical links obtained by percolation theory and edge centrality are compared and integrated to determine the final critical links. The detailed methodology will be presented in the Research Methodology section.

### B. RESEARCH CONTRIBUTION

This work suggests a complex network perspective towards spatial-temporal critical links detection in airway networks. The research highlights are summarized as follows.

- 1) We adopted two network approaches, i.e., percolation theory and network centrality, for dynamic critical links detection in spatial-temporal airway networks constructed from real flight data. Compared to many existing methods that only consider a single metric, such as network centrality metric, the proposed method combines two metrics that identify the critical links from both airway network structure and air traffic structure perspectives using real traffic data. Moreover, existing studies for critical links detection primarily deal with static networks that do not fit airway net-



**FIGURE 1:** A graphical illustration to the proposed research problem of detecting critical links in a given airway network by making use of complex network theories.

works due to their time-evolving nature under different traffic situations.

- 2) We verified the efficacy of the proposed critical link identification method from three perspectives: 1) air traffic volume perspective, i.e., the ratio of flights in SEAN transiting through the identified critical links; 2) airspace design perspective, i.e., positions of the identified critical links on trunk jet routes and their connections to key navigational aids; 3) operational perspective, i.e., a spatial view based on both airspace as well as traffic flow structures, and a temporal view based on varying traffic scenarios.
- 3) We further visualized the real-time movements of flights and the dynamic changes of critical links over time. Observations made by Subject Matter Experts (SMEs) from the traffic visualization demonstrated that the network-theory-based method could dynamically identify critical links which are operationally critical in fact.

## IV. RESEARCH METHODOLOGY

### A. METHODOLOGY OVERVIEW

As can be seen from Fig. 1, the proposed method for critical link detection contains three key steps: spatial-temporal network modelling, critical links detection based on network theories, and final critical links determination.

Given the flight track data during a specific time, the network modelling step constructs spatial-temporal airway networks based on the flight fixes and flight paths. Besides, the normalized average flight speed on each link in an airway network is determined and is taken as the weight for the corresponding link.

The critical links detection step works on the constructed spatial-temporal airway networks. This step will leverage two network methods, i.e., edge centrality metric and percolation theory, to detect critical links from each network snapshot. For each network snapshot, the critical links detection step is likely to yield different critical links. The critical links determination step is to compare and analyse all the detected

critical links and merge them to filter out the final critical links for the studied airway network.

### B. NETWORK MODELLING

The purpose of network modelling is to construct the weighted spatial-temporal airway networks for the critical links detection step. Network modelling consists of two steps, namely, extract the airway network configuration and determine the weight on each link from the flight track data. In this study, we use the normalized average ground speed instead of the number of aircraft on each link as its weight. The main reason is that buffer time for airborne congestion as well as the risk of delay propagation through the entire airway network can be reduced if flights can faster transit through their routes [39]. Moreover, when an airway link is faced with congestion or other disruptions, major reactive measures in operational air traffic flow management (ATFM) are flights vectoring and speed adjustment [40]. These measures will consequently influence the speed of flights transiting through the affected links. The travel speed on a link is normalized using the daily maximum speed. Therefore, the lower weight of a link indicates that the current traveling speed on the link is more degenerated than the best daily traffic situation.

The flight track data required for network modelling includes the flight paths of each flight, i.e., the flight fixes of the flight trajectory and the time when the flight is reported to be at these fixes. From the flight path information, we will be able to construct the airway network configuration by setting the flight fixes as the nodes and determining the connections between nodes, i.e., links, from the path of each flight. If there are flights whose paths pass the link between two nodes, the two nodes will be considered as connected. Consequently, there will be a link connecting the two nodes on the resulted airway network. In this manner, the airway network will be constructed entirely from the flight track data.

With the time information of flights reaching the fixes, the average speed  $s_{a,j}$  of a flight  $f_a$  on the link  $e_j$  of its path can be computed by averaging the length  $L_j$  of  $e_j$  over the flight duration  $T_j^a$  on  $e_j$ :

$$s_{a,j} = \frac{L_j}{T_j^a} \quad (2)$$

Note that we are identifying critical links for the  $k^{\text{th}}$  time period  $T_k$  (from  $t_k^0$  to  $t_k^1$ ), therefore the required weight  $w_j$  on link  $e_j$  is the normalized average flight speed of all flights passing  $e_j$  during  $T_k$ , instead of simply normalizing the average flight speed of all flights passing  $e_j$ . This means that for flight  $f_a$ , only the part  $l_{a,j}^k$  on  $e_j$ , that has been flown during  $T_k$ , will be considered, so we cannot simply take the mean of the average flight speed  $s_{a,j}$  of all flights on link  $e_j$ . From the available traffic data, it is not able to obtain the exact time line of flight  $f_a$  when it is on  $e_j$  during  $T_k$ . Therefore, to reduce the bias, we assume that the flight  $f_a$  is flying on  $e_j$  with the constant speed  $s_{a,j}$ . Then, given the entry time  $t_{en}^{a,j}$  and exit time  $t_{ex}^{a,j}$  of  $f_a$ , the flight duration  $T_{a,j}^k$  of  $f_a$  on  $e_j$  during  $T_k$  can be determined:

$$T_{a,j}^k = \min\{t_{ex}^{a,j}, t_k^1\} - \max\{t_{en}^{a,j}, t_k^0\} \quad (3)$$

Then,  $l_{a,j}^k$  can be estimated as  $L_j$  weighted by the proportion of  $T_{a,j}^k$  to  $T_k$ :

$$l_{a,j}^k = \frac{L_j \times T_{a,j}^k}{T_k} \quad (4)$$

The average speed  $s_j^k$  on link  $e_j$  during  $T_k$  can be calculated by averaging the sum of flight distances of all the flights on  $e_j$  over the according sum of flight duration:

$$s_j^k = \frac{\sum_{a=1}^F l_{a,j}^k}{\sum_{a=1}^F T_{a,j}^k} \quad (5)$$

where  $F$  is the total number of flights passing link  $e_j$  during  $T_k$ .

Finally, the weight  $w_j$  on link  $e_j$  during the given time period  $T_k$  is determined by normalizing the average speed  $s_j^k$  with the daily maximum speed  $s_{max}^j$  on link  $e_j$ :

$$w_j = \frac{s_j^k}{s_{max}^j} \quad (6)$$

In this way, the weight on link  $e_j$  is determined, which will be a number between 0 and 1.

### C. CRITICAL LINKS DETECTION

To measure how critical an edge of a network is, we adopt two methods from the viewpoint of network theory. The first method is to make use of the edge centrality metric. The second method is based upon network percolation theory.

#### 1) Centrality Method

Centrality is a class of straightforward metrics for quantifying the importance of a network's components. For a given airway network, we use Eq. 1 to calculate the centrality for each link. Note that there exist a couple of edge centrality metrics in the literature. In this work, only the betweenness centrality metric is adopted. The main reason is that the

betweenness centrality is involved with the shortest paths in a network which is more appealing to airway networks.

After getting the centralities of the edges, we then rank the edges based on their centralities. Edges with the highest centralities are regarded as critical links. Specifically, the top  $K$  are taken as the critical links. In the experiments, we set  $K = 10$ . Note that  $K$  cannot be too large as it would not be possible for an airway network to have too many critical links. Also,  $K$  cannot be too small as the detection results need to compare in the subsequent analysis with what is detected by using the percolation theory.

#### 2) Percolation Based Method

Percolation theory has been widely applied to investigate the structural properties of diverse complex networks, including transportation networks. For example, the authors [14] introduced percolation theory to detect critical links in urban traffic networks. Percolation theory uses statistical physics principles and graph theory to analyse changes in the structure of a complex network subject to perturbations. The percolation threshold  $p_c$  signifies the transition point of a given network, thus, shedding light on probing its critical sub-structures.

##### 1) Critical Threshold Identification

Inspired by network percolation theory, we carry out an experimental study on a given airway network. Note that the lower weight of a link means that the current traveling speed on the link is more degenerated than the best daily flight speed on this link. Therefore, these lower-weight links can be regarded as failed links which can potentially slow down the flights and induce congestion. By incrementally closing these low weight links, we will observe the links whose closure will lead to a transition of the airway network from the phase of connected to the phase of disconnected.

Note that an airway link  $E_j$  is characterized by the weight  $w_j$ . Therefore, for a given threshold of  $q \in [0, 1]$ , the link  $E_j$  can be classified into two categories: functional when  $w_j \geq q$  and dysfunctional when  $w_j < q$ . This can be represented as:

$$E_j = \begin{cases} 1, & w_j \geq q \\ 0, & w_j < q \end{cases} \quad (7)$$

As the value of  $q$  increases, more low-weight links are closed, which makes the network sparser. Note that the weight on a link refers to the normalized average flight speed on that link. It indicates that as  $q$  increases, links with low flight speeds are closed, and links with higher flight speeds remain active. In this way, a functional airway network can be constructed for a given  $q$  value according to the traffic dynamics of the original airway network.

As  $q$  increases, the original network will be disintegrated into several isolated clusters because of the closure of some low speed links. Therefore, the size of the largest cluster decreases, and the second-largest cluster reaches a maximum at the percolation threshold  $q_c$  which is the transition to the disconnected phase from the connected phase of an airway

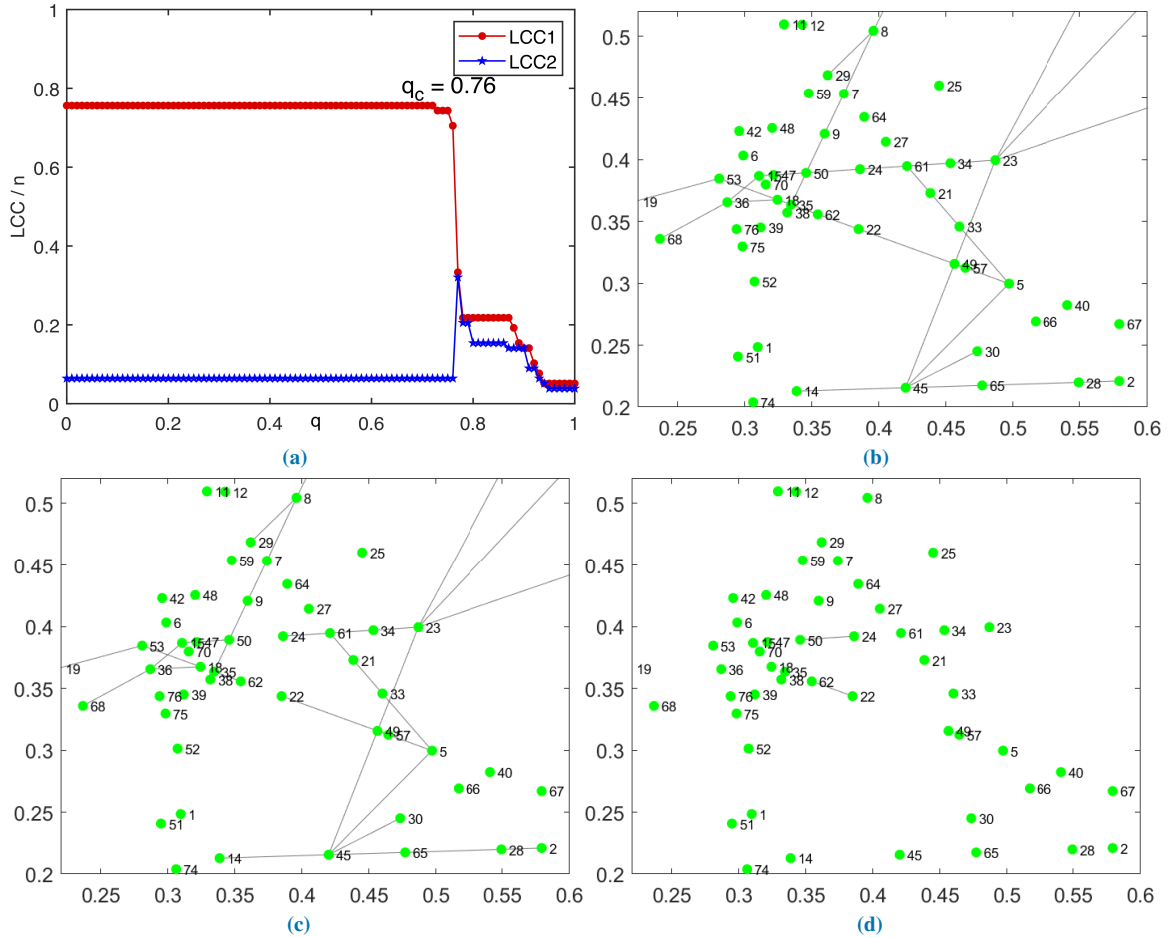


**FIGURE 2:** Percolation process on the SEAN. (a) The relative sizes of LCC1 and LCC2 are shown as a function of  $q$ . The sudden decrease of the size of LCC1 and the increase of the size of LCC2 indicates that, at the percolation threshold  $q_c$ , LCC1 is broken into several isolated clusters because of the closure of some links. Therefore, the network transits from a largely connected phase to a disconnected phase at  $q_c$ . The LCC1 of the SEAN (b) at and (c) after the critical threshold  $q_c$  with respect to the percolation process. (d) The critical links with respect to the critical threshold  $q_c$ . Each node number represents a unique node in the network.

network, as shown in Fig. 2a. The y-axis of Fig. 2a refers to the fraction of the size of the largest connected component (LCC1) or the second-largest connected component (LCC2), which is a value between 0 and 1.

As an indicator of the robustness characteristics of network connectivity [41], the percolation threshold  $q_c$  in this percolation process quantifies the organization efficiency of real air traffic. Flights can travel to most nodes in the airway network (the largest connected component of airway network) with normalized speed below  $q_c$ , while flights will be trapped in small isolated clusters when they fly with normalized speed above  $q_c$ . Hence,  $q_c$  measures effectively the maximum normalized speed with which flights can travel over a large part of the airway network, which reflects the global efficiency of air traffic from a network perspective.

## 2) Critical Links Identification

At the critical threshold  $q_c$ , LCC1 of an airway network exists, and LCC2 is relatively small in size. As reflected in Fig. 2a, when more links are further removed from LCC1, then LCC1 will break down into small pieces. As a consequence, the size of LCC2 grows. Fig. 2b further takes SEAN

as an example to better show this point.

Fig. 2b displays the structure of LCC1 of a weighted SEAN at the critical threshold  $q_c$  with respect to the percolation theory. In Fig. 2c, LCC1 fragments into pieces after  $q_c$  due to the removal of the critical links. Fig. 2d shows the critical links. The critical links are identified as follows:

$$E_c = \{e \in E \mid w_e < q_c + \delta\} \quad (8)$$

in which  $\delta$  is the interval for the variation of variable  $q$ ,  $q \in [0, 1]$ .

## D. CRITICAL LINKS DETERMINATION

For each snapshot  $G^{t_i}$  of the constructed spatial-temporal networks, there are two sets of detected critical links, one yielded by centrality metric and the other one by percolation theory. Note that edge betweenness centrality helps to identify links that act as the traffic pivots with which shortest paths frequently pass through, while percolation theory identifies links that act as the bridges whose failures will decrease the network's structural integrity significantly.

Links identified by both percolation theory and betweenness centrality can meet the requirements of critical links defined in this paper, i.e., pivot links contributing to shortest flight paths and bridge links contributing to structural integrity. Therefore, we take the overlapped links of the two link sets, which are identified respectively by betweenness centrality and percolation theory, as the final critical links  $E_c^{t_i}$  of  $G^{t_i}$ .

The critical links  $E_c^{t_i}$  are identified for time period  $t_i$ . Note that the critical links will evolve over time following different traffic situations. This critical link determination process will dynamically provide critical links for different periods. By observing the changes of critical links, temporal distribution of the critical links can be obtained. We further merge  $E_c^{t_i}$  across the time horizon to get the critical links for the original airway network  $G$ . By doing so, a holistic view of the spatial distribution of the critical links for a given airway network can be achieved.

## V. EXPERIMENTAL STUDY

### A. NETWORK MODELLING

The above section describes the proposed method for critical links detection in an airway network with given flight track data. To check the efficacy of the proposed method, in this section, we carry out a case study on the SEAN. SEAN sits on the juncture of six neighboring FIRs and covers south China sea airspace, where most of the air traffic from China converges towards South-East Asia. Despite its small size, it has features of various airspace, e.g., radar, procedural, and oceanic. Moreover, SEAN has complex traffic structures comprising the confluence of en-route air traffic from neighboring airspace, climbing traffic from the terminals, descending traffic to the terminals. The complexity in the traffic structure and the high traffic demand are likely to induce air traffic congestion during peak hours, making it significant to detect critical links in such an airway network. The network structure of SEAN is shown by blue lines in Fig. 3a. The black dashes represent the sector boundaries of Singapore FIR.

The SEAN shown in Fig. 3a consists of 118 nodes and 174 links. In the experiments, one-month (1st Dec. 2018 to 31st Dec. 2018) en-route flight track data provided by the Civil Aviation Authority of Singapore is used. December is the peak season for air transportation due to the increasing travel demand during the holiday. During this period, the high traffic demand provides the advantage and possibility to reveal the critical links in airway networks which significantly affect the network's performance in terms of structural integrity, functionality, etc. The tested one-month data records the information of 44215 flights, including flight fixes and the time passing those fixes.

Based on the one-month flight track data, we further construct the weighted spatial-temporal airway networks. Note that the distributions of the critical links may change over time. Therefore, the spatial-temporal airway networks are constructed over time for different time slots. Fig. 3b displays

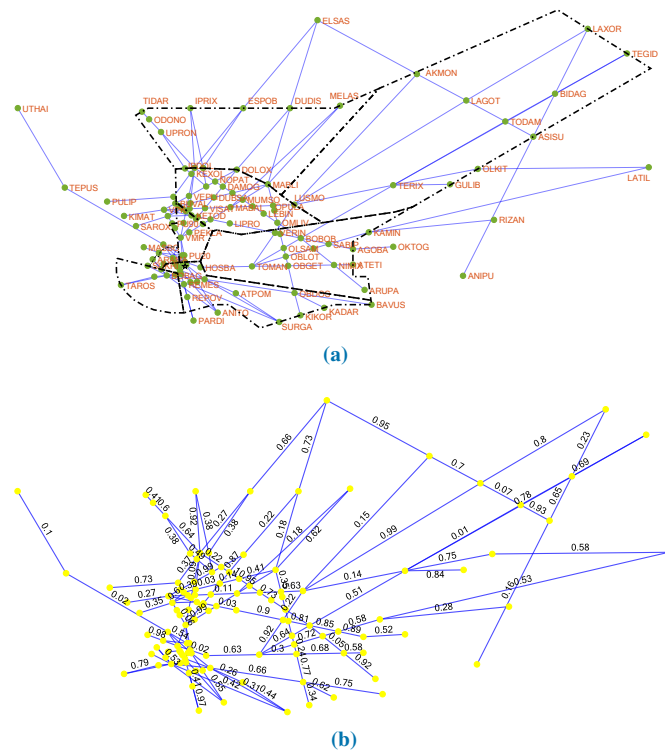


**FIGURE 3:** The network structure of (a) SEAN with spatial information. The black dashes represent the sector boundaries of Singapore FIR, and the green nodes represent the waypoints whose names are shown in red letters and (b) the weighted SEAN with the weights being the normalized average flight speed on the links.

a snapshot of the weighted spatial-temporal airway networks for SEAN during a 30-minute time slot.

### B. CRITICAL LINK DETECTION

To study the evolution of critical links overtime under different traffic situations, spatial-temporal networks are constructed for different time slots characterizing the evolution of traffic situations. Moreover, the length of the time slots chosen may influence the critical links detection outcome. Therefore, in the experiments, the weighted spatial-temporal airway networks are constructed with different time scales. Expressly, we respectively set the time scales to be 15 minutes, 30 minutes, 45 minutes, and 60 minutes, resulting in four sets of spatial-temporal networks. The reason for adopting the four time scales between 15 to 60 minutes is that “15-minute” and “60-minute” (1 hour) are the commonly used horizons for evaluation of controllers’ workload and air traffic planning purpose [42]–[45]. For example, in the MAP (Monitor Alert Parameter) model, the airspace capacity is computed on a 15-minute basis [46]. For the one-month en-route flight track data from 1st Dec. 2018 to 31st Dec. 2018, there will be 2976, 1488, 992, 744 weighted networks constructed over time when the time scales are set as 15 minutes, 30 minutes, 45 minutes and 60 minutes, respectively. Then the critical links Will be detected from each set of the networks using both percolation theory and edge betweenness centrality metric.

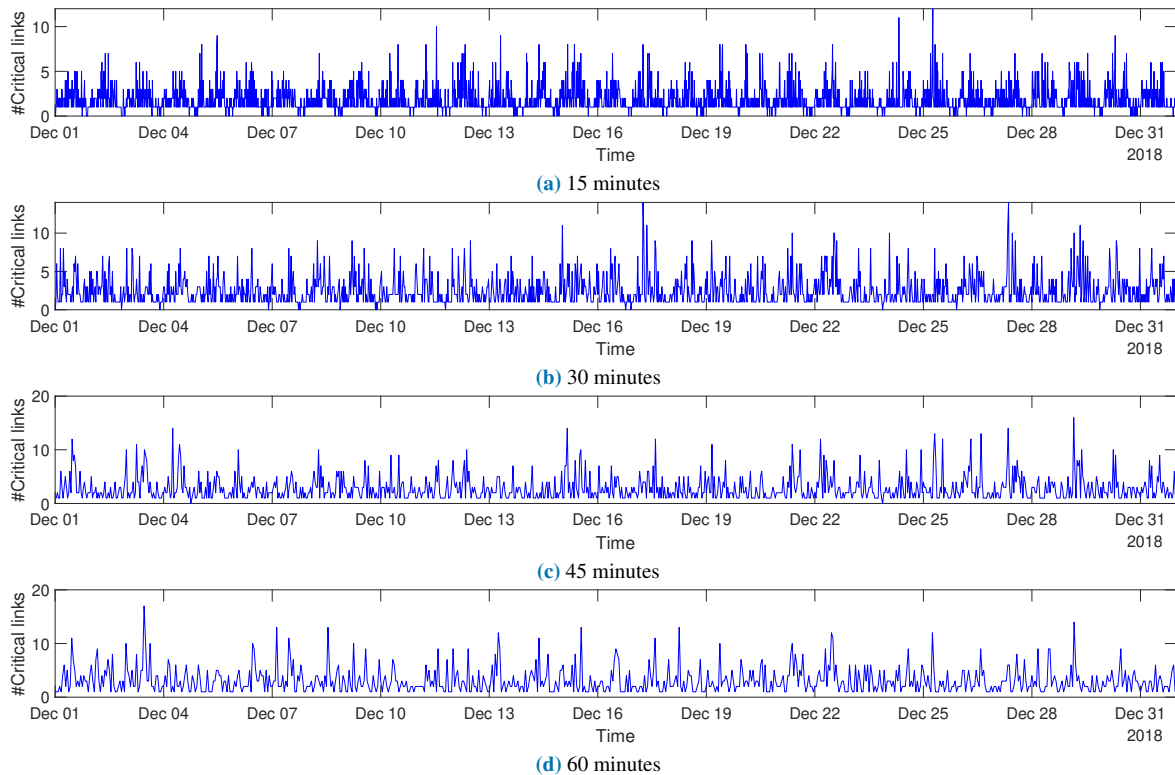


**FIGURE 4:** The number of critical links detected from 1st Dec. 2018 to 31st Dec. 2018 using the percolation theory applied to the spatial-temporal SEAN with different time scales. The average number of critical links detected for each snapshot under 15 minutes, 30 minutes, 45 minutes and 60 minutes are 1.9543, 2.5673, 2.8697 and 3.1116 respectively.

#### 1) Variations of the Number of Critical Links

As mentioned in Section IV-C1, for the centrality metric, we always choose the top 10 links with the highest centrality values

to be the critical links of each weighted network. Therefore, here we first analyze the variations of the number of critical links over time, detected by using percolation theory.

Fig. 4 visualizes the temporal distribution of the number of critical links detected by using network percolation theory. In the percolation studies, we set the interval  $\delta$  for the variation of variable  $q$ ,  $q \in [0, 1]$ , to be  $\delta = 0.001$ . The curves in Fig. 4 show that the number of detected critical links varies over time. However, the maximum number does not exceed 18, while the average number of critical links detected for each snapshot under 15 minutes, 30 minutes, 45 minutes and 60 minutes are 1.9543, 2.5673, 2.8697 and 3.1116, respectively.

It can be observed from Fig. 4 that as the length of the time slot for constructing the temporal networks increases from 15 minutes to 30 minutes, 45 minutes, and 60 minutes, there is also a slight increase in the number of the critical links identified. The possible reason could be that the fluctuations in the traffic situation on some links and the influence of a single link over the network percolation process are neutralized when the time span of traffic data to construct the weighted network increases.

Moreover, we can observe from Fig. 4, especially from Fig. 4(a), that the number of identified critical links seems to change cyclically daily. The troughs in the curve usually

appear from 18:00 UTC to 23:00 UTC, especially around 21:00 UTC. From 23:00 UTC to the following 18:00 UTC, some peaks in the identified critical links show up. The reason for such a phenomenon is likely to be hub airport nature of Singapore Changi airport. This oscillatory behaviour of the number of identified critical links is due to hub-nature of Singapore Changi Airport. An overview of the hourly level of activity of Singapore Changi Airport reveals distinct patterns related to its connectivity. Changi airport acting as a hub (the airport as an intermediary location) has several noticeable surges of activity during the day. Surges at hub airports are often characterized by several inbound flights arriving within a time-frame, and about 2 hours later, a surge of outbound departures can be observed. For most hub airports, there is a peak of activity around 7 AM and another peak around 7 PM, which mostly corresponds to short-haul flights and preferences for passengers to depart in the morning and return in the evening.

#### 2) Spatial Distribution of the Detected Critical Links

For different network snapshots, the detected critical links could be unique. Therefore the spatial distributions of the detected links are further compared. Specifically, for each critical links detection metric, i.e., network percolation and edge betweenness, the critical links detection results in each weighted network are integrated by counting up the frequencies of each link being detected as critical in all time slots. The corresponding results are shown in Fig. 5.

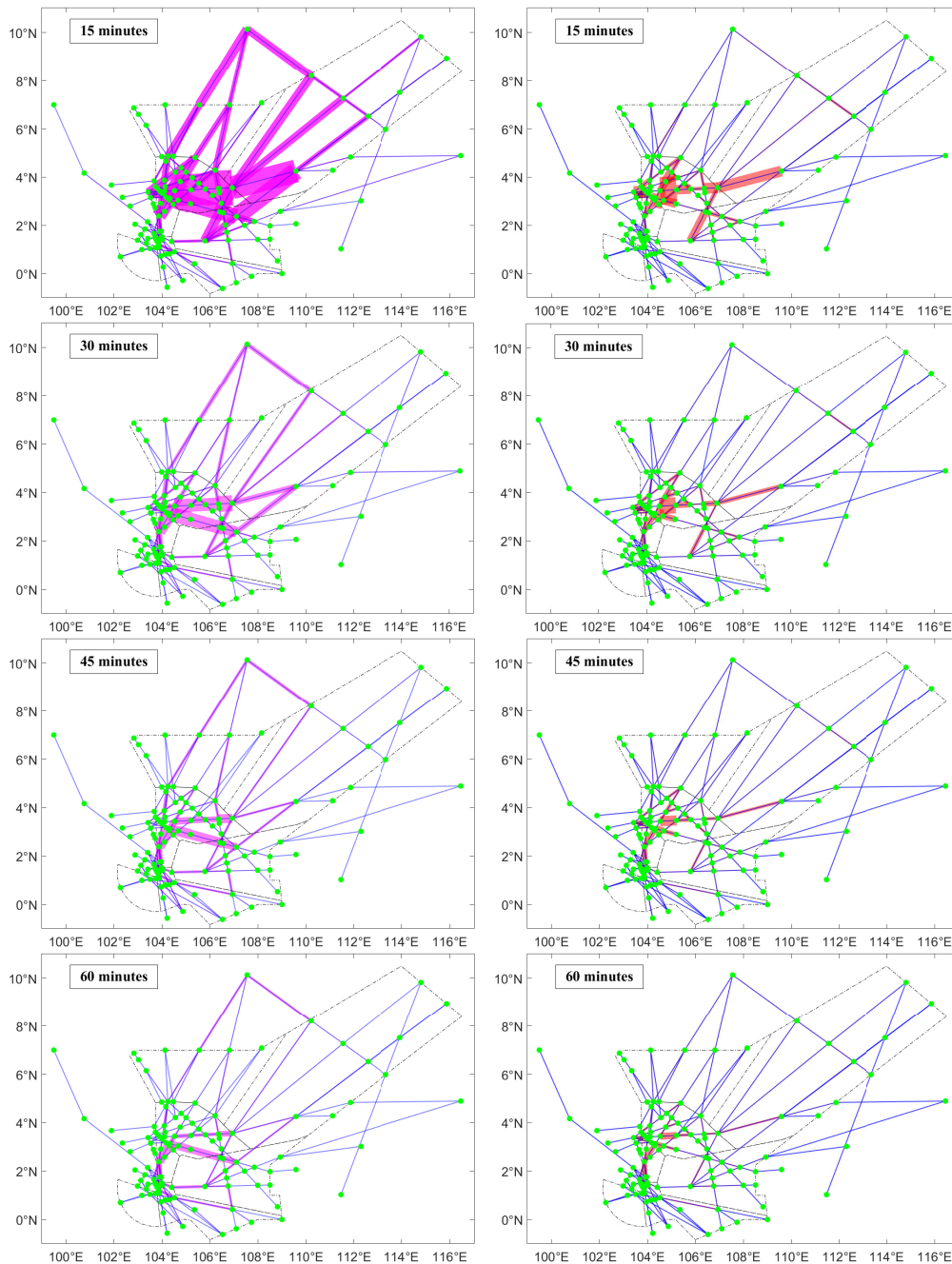


**FIGURE 5:** Critical links detected using the betweenness centrality metric (left column) and percolation theory (right column) when applied to the spatial-temporal networks with different time scales. The purple (left column)/red (right column) links are the determined critical links, and the link thickness is proportional to their frequencies being identified as critical links over time.

Fig. 5 shows that the frequencies of the critical links detected by using the centrality metric are relatively higher than that of percolation theory. The reason is that there are ten critical links for each network snapshot when the centrality metric is of concern. While using percolation theory, the average number of critical links detected for each snapshot is 2 to 3. Whichever method is used, Fig. 5 demonstrates that only a small portion of the detected critical links have relatively high frequencies.

Fig. 5 presents the detected critical links that vary in numbers and detection frequencies for the time slot for constructing the corresponding spatial-temporal weighted networks. It can be observed that as the time scale of network snapshots increases, the frequency of the detected critical links decreases (thickness of the red/purple links reduces). The main reason is that when the time scale increases, fewer network snapshots will be constructed based on the one-month traffic data. A short time slot captures the air traffic

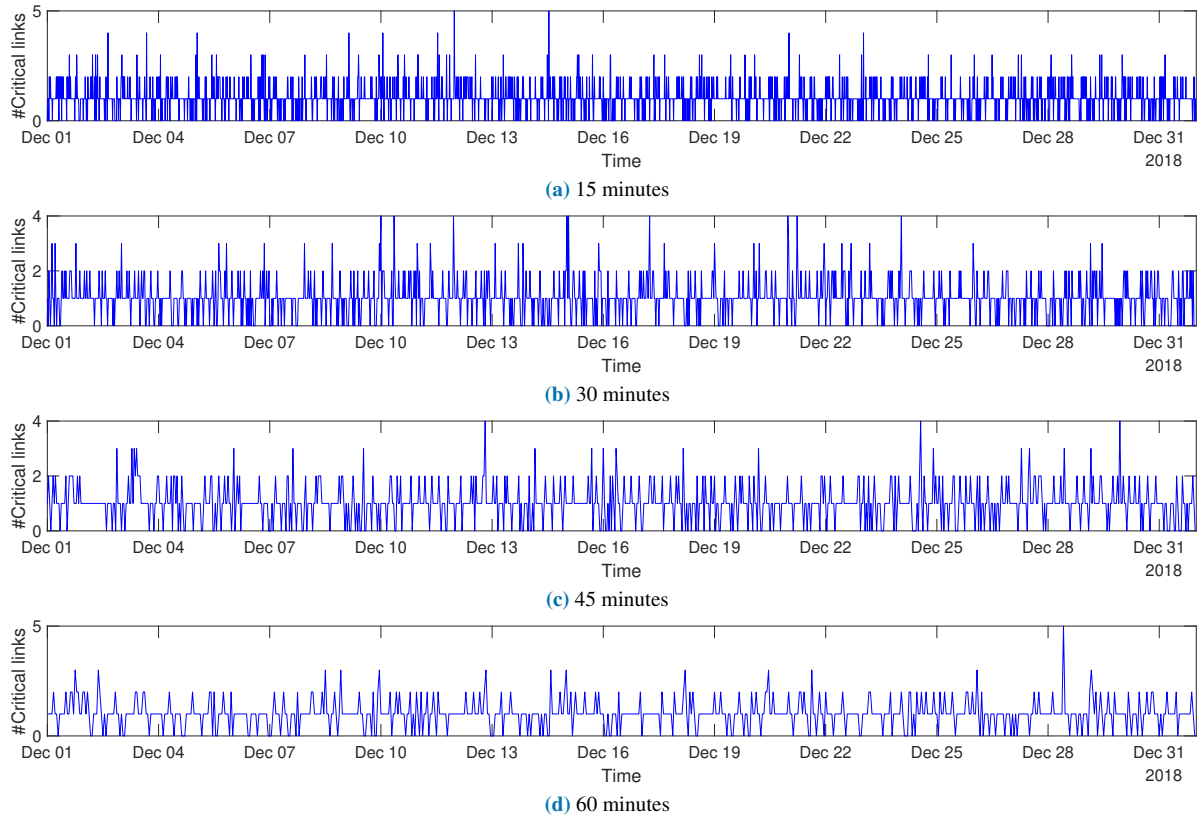


**FIGURE 6:** The number of the final critical links determined from 1st Dec. 2018 to 31st Dec. 2018 in the spatial-temporal SEAN modelled with different time scales, i.e., 15 minutes (a), 30 minutes (b), 45 minutes (c) and 60 minutes (d).

within a short time window, thus providing a microscopic view to investigate the network dynamics. A long time slot gauges the air traffic over a long period, providing a macroscopic view of the network dynamics. There is no need to fix the time slot when constructing the temporal networks. As a result, a decision-maker can choose a proper time granularity concerning a specific task and purpose.

The above experiments mainly demonstrate overall comparisons between the spatial distributions of the critical links detected by the two network metrics as it is difficult to compare the structural difference at each period. In what follows, we present the critical link determination results.

### C. CRITICAL LINK DETERMINATION

#### 1) Number of Determined Critical Links

At each time period, we determine the critical links for the corresponding network snapshot as the overlapped links of the two critical link sets that are detected respectively using the two network metrics. The variation of the number of final critical links for the network snapshots over time is recorded in Fig. 6.

By comparing Figs. 4 and 6 we can notice that the number of critical links determined for each network snapshot reaches a reasonable level after overlapping the critical links determined using network percolation metric and edge betweenness centrality. We also can observe from Fig. 6 that,

under some time slots, multiple critical links exist, while under some slots, only one critical link or no critical link is identified.

#### 2) Temporal Distribution of Determined Critical Links

The proposed network approach can detect the critical links in a given airway network both spatially and temporally. Fig. 7 demonstrates the temporal distribution of the determined critical links in the SEAN. In Fig. 7, the X-axis represents the link ID of the 174 links in the SEAN, while the Y-axis represents the time. More specifically, the X-axis view of Fig. 7 shows the exact links out of the 174 links that have been detected as critical for a given time horizon, while the Y-axis view of Fig. 7 presents the criticality evolution (critical or non-critical) of a specific link over time. The black block (ID, time) illustrates that the link with the corresponding ID on the X-axis has been identified as a critical link at the corresponding time on the Y-axis.

It can be observed from Fig. 7 that there exist four common links which are frequently being identified as critical. These links are (identified by entry-exit waypoints) as follows: “MABAL – VISAT”, “RAXIM – VMR”, “KILOT – OT-LON”, and “KILOT – LIPRO” (marked with red arrows and their corresponding names).

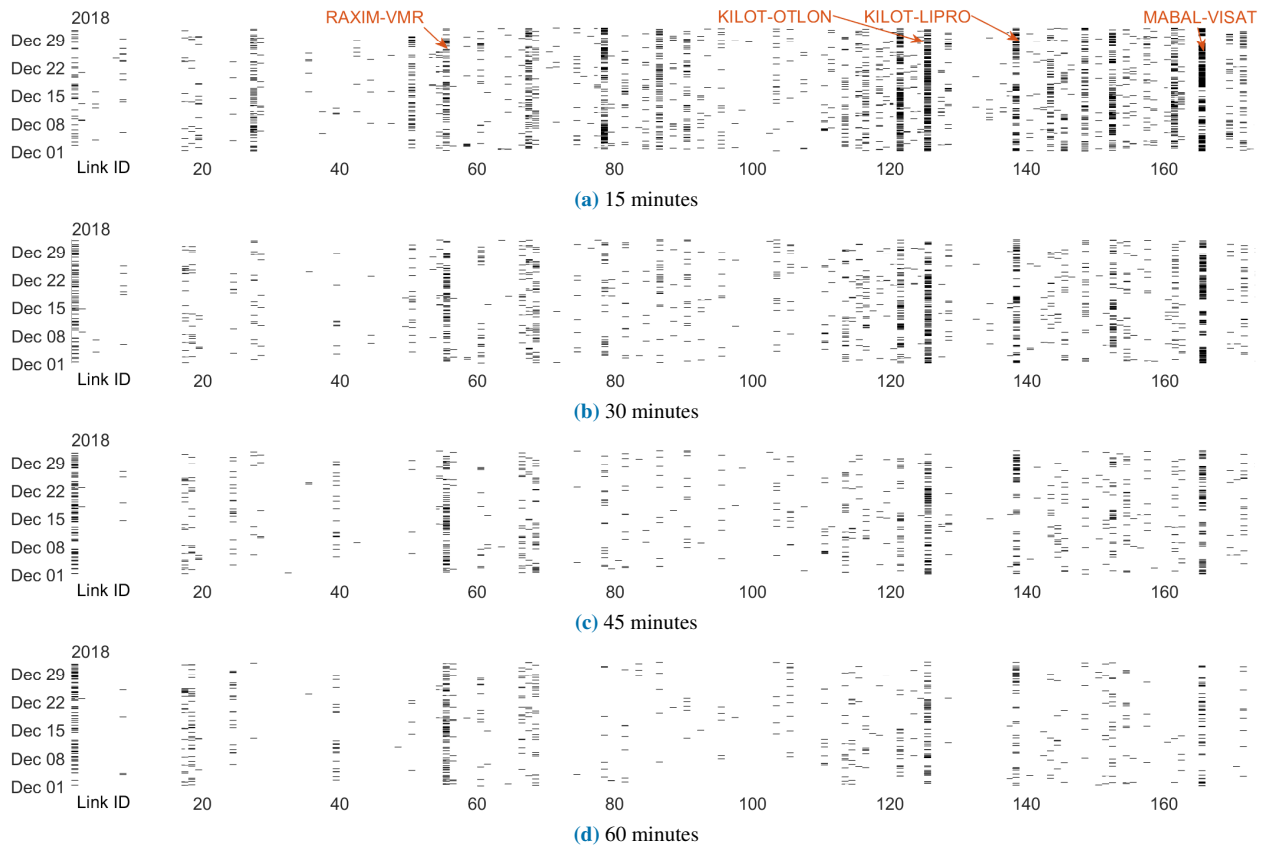


**FIGURE 7:** Critical links identified over time under different time scales (i.e., 15 minutes (a), 30 minutes (b), 45 minutes (c) and 60 minutes (d)) in modeling the spatial-temporal networks. The variable on X-axis, ranging from 1-174, represents the 174 links in SEAN, while the variable on Y-axis represents the time from 1st Dec. 2018 to 31st Dec. 2018. When a link (whose coordinate is  $x$  on the X-axis) is identified as critical during a time period (whose coordinate is  $y$  on the Y-axis), the corresponding area of the coordinate ( $x, y$ ) will be marked as a black block.

### 3) Spatial Distribution of Determined Critical Links

Fig. 8 visualizes the spatial distributions of the final determined critical links in the SEAN. The red links are the determined critical links, and the thickness of the links is proportional to their frequencies.

We can see from Fig. 8 that the majority of the critical links are located in the sector highlighted in purple. This sector is the most loaded in the airspace covered by SEAN, within which traffic complexity and density are distinctly higher than other sectors [47]. Also, it can be observed that as the time scale of network snapshots increases, the number of detected critical links together with their frequencies decreases (thickness of the red links reduces). Two reasons are attributable to this phenomenon. First, fewer network snapshots will be constructed based on the one-month traffic data when the time scale becomes larger. Therefore, the frequencies decrease as there are fewer network observations. Second, each spatial-temporal network snapshot is constructed based on the traffic for a given time period. If the time scale for constructing the weighted networks becomes larger, then the weights on the airway links do not distinguish from each other, resulting in homogeneous network observations. Consequently, both the centrality metric and the percolation

theory will not work for a homogeneous network as each link in the network acts importantly the same as others do.

### D. VALIDATION ON THE IDENTIFIED CRITICAL LINKS

The above experiments have demonstrated the case study on the critical links detection in the SEAN using the suggested network theories. In this section, we validate the criticality of the detected critical links from three perspectives.

#### 1) Air Traffic Volume Perspective

One can see from Fig. 6 that the maximum number of detected critical links in the SEAN is 5. Note that there are a total number of 44215 flights passing through the SEAN in Dec. 2018. The ratio of flights passing each of the five critical links, appearing with the highest frequency under different time scales, over the total number of flights is presented in Table 1.

Note that the four links marked in bold in Table 1 are the commonly identified critical links under different time scales. It can be observed from Table 1 that the four links have high relative usages by flight as the ratios of being transited through by flights are large. If anyone of the four links is blocked due to weather or airspace restriction, the

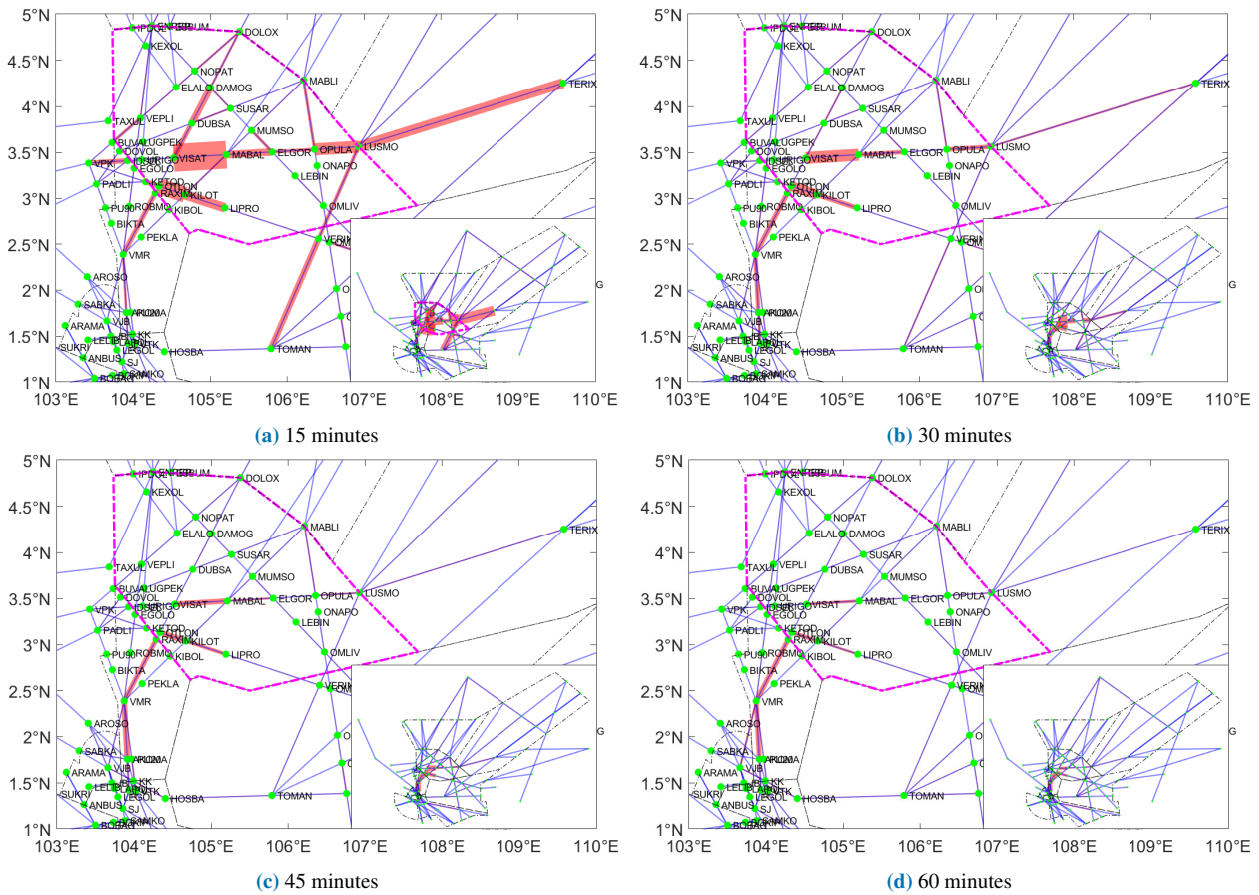


**FIGURE 8:** Spatial distributions of the critical links in SEAN. The red links are the determined critical links, and the thickness of the links is proportional to their frequencies.

**TABLE 1:** Ratio of flights ( $r$ ) on each of the 5 high frequency links being detected as critical links under different time scales.

15minutes		30minutes		45 minutes		60 minutes	
Link Name	$r$ (%)						
MABAL – VISAT	10.68	MABAL – VISAT	10.68	KILOT – OTLON	5.68	RAXIM – VMR	5.69
KILOT – OTLON	5.68	KILOT – OTLON	5.68	AKOMA – VMR	13.37	AKOMA – VMR	13.37
LUSMO – OPULA	10.69	RAXIM – VMR	5.69	MABAL – VISAT	10.68	KILOT – OTLON	5.68
LUSMO – TERIX	9.90	KILOT – LIPRO	5.68	RAXIM – VMR	5.69	MABAL – VISAT	10.68
KILOT – LIPRO	5.68	LUSMO – OPULA	10.69	KILOT – LIPRO	5.68	KILOT – LIPRO	5.68

corresponding portion of flights as recorded in Table 1 will be directly affected. For example, if the link “MABAL – VISAT” is blocked, 10.68% of the total flights will therefore be affected, and air traffic control operations such as flight re-routing, speed control, vectoring, etc., would be required.

2) Airspace Design Perspective

Jet routes are equipped with ground-based navigation beacons such as VOR/DME stations. A VOR/DME beacon emits radio signals to provide surveillance information (range and bearing) for flights to navigate through the sky [48], [49]. VOR/DME stations serve as important navigational aids connecting all significant traffic flow sources [50]. Fig. 9 presents a snapshot of the aeronautical chart of SEAN in which the

four high-frequency critical links are annotated.

It can be seen from Fig. 9 that the three links “MABAL – VISAT” (on airway M758), “KILOT – LIPRO” and “KILOT – OTLON” (on airway M761) lie on airways (radio signals) radiated from PEKAN VOR/DME, which pilots and controllers will primarily choose for easy use of navigation. Moreover, links “KILOT – LIPRO” and “KILOT – OTLON” are on airway M761 between the outbound radio of two VOR/DMEs (PEKAN VOR/DME and KUCHING VOR/DME). This airway serves the heavy traffic between Kuala Lumpur (in west Malaysia) and Kuching (in East Malaysia) [51]. Link “MABAL – VISAT” is on the airway from PEKAN VOR/DME to waypoint “LUSMO”, the metering point for flights entering sector 5 in Singapore airspace

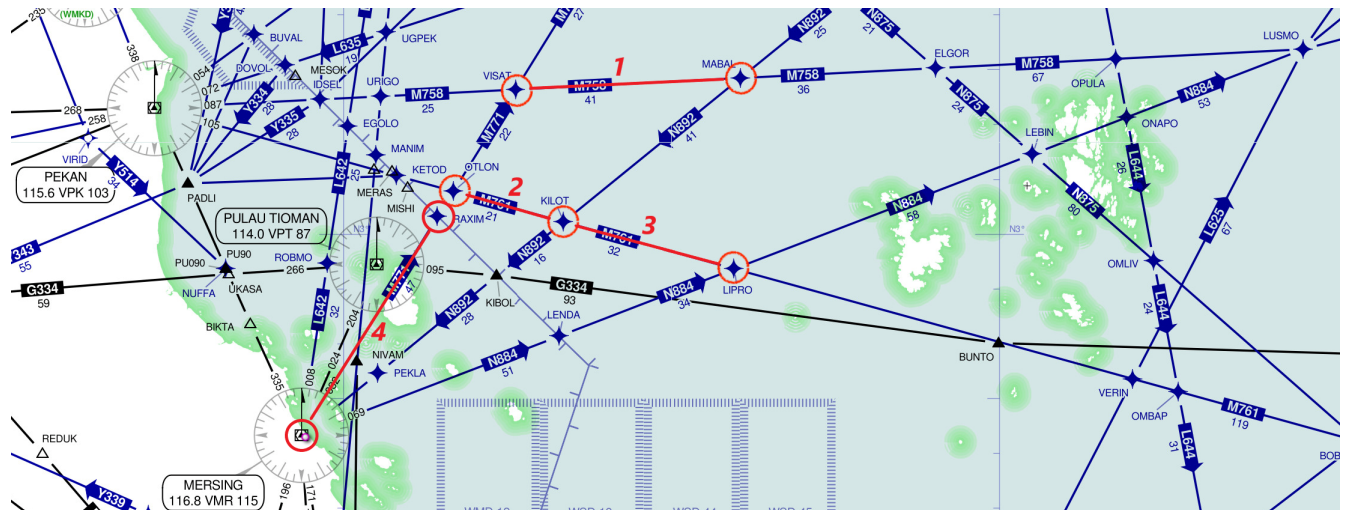


**FIGURE 9:** Geographical positions of critical links 1 - “MABAL – VISAT”, 2 - “KILOT – OTLON”, 3 - “KILOT – LIPRO” and 4 - “RAXIM – VMR”. The picture is excerpted from the website of SkyVector [52].

fly to Indonesia, Philippines, East Malaysia, and Japan. Waypoints “MABAL”, “VISAT”, “OTLON”, “KILOT”, and “LIPRO” are the crossing points for airways radiated from MERSING VOR/DME and PEKAN VOR/DME, which serves major air traffic flows from airports in Singapore and Malaysia. Link “RAXIM – VMR” caters to the heavy traffic flow between Singapore and China. Waypoint “VMR” is at MERSING VOR/DME, which is a crucial metering point for flights from/to Singapore airports. Additionally, apart from the four links, the rest of the seven links listed in Table 1 (“LUSMO – OPULA”, “LUSMO – TERIX”, and “AKOMA – VMR”), are all located on airways radiated from VOR/DMEs.

### 3) Operational Perspective

This section presents the validation of the criticality of the identified links from an operational perspective, considering the feedback from operational experts. The detection results are validated from an operational perspective, including i) spatial view based on airspace and traffic flow structures, and ii) temporal view based on real traffic scenarios.

#### i) Spatial view based on airspace and air traffic flow structures

Table 2 summarizes the characteristic information of the four critical links “MABAL – VISAT”, “KILOT – OTLON”, “KILOT – LIPRO” and “RAXIM – VMR”. SMEs use this information to analyse the spatial criticality of the identified critical links. In the following paragraphs, the analysis of each of the four links will be illustrated one by one.

**1) Spatial criticality of link “MABAL – VISAT”:** Airway link “MABAL – VISAT” is located on Air Traffic Service (ATS) route M758, which is a bidirectional airway. It accommodates high traffic volumes as the ratio of flights in SEAN transiting through “MABAL – VISAT” is 10.68%. Given the short length of the link, which is 41 nautical miles (nm), “MABAL – VISAT” possesses a high traffic density while

the peak number of aircraft transiting through the link is 6 ~ 7 per 15 minutes derived from the traffic data.

Table 2 lists the Entry – Exit waypoints, in SEAN, of flights transiting through “MABAL – VISAT”. The right-heading arrow indicates that the flights are transiting in the direction presented in the table header, i.e., “MABAL – VISAT”, and vice versa. The corresponding flight paths, connecting these Entry – Exit pairs of flights transiting in the direction of “VISAT – MABAL”, are highlighted by green dashes in Fig. 10, while paths in the direction of “MABAL – VISAT” are highlighted by green dashes in Fig. 11. It can be seen from Fig. 10 that flights flying outbound of Singapore FIR and taking the three major ATS routes, namely, L625, N884, and M758, will transit through the link in “VISAT – MABAL” direction. The ATS route of M758 facilitates the smooth flow of heavy air traffic between Peninsular Malaysia and East Malaysia, Brunei [53]. Air traffic on ATS route M758 handles approximately 742 movements a week in 2016 [53]. The unidirectional ATS routes N884 and L625 cater to the main traffic flow flying eastbound to the Philippines, far east (Japan), USA, etc [51]. Fig. 11 shows that inbound flights, from Peninsular Malaysia, Brunei, Philippines and far east via ATS routes M767 (unidirectional), M758 (bidirectional), merge to route M758 and transit through link “MABAL – VISAT” to the west. From this point of view, the critical link “MABAL – VISAT” serves as a pivot to spread the eastbound flights in SEAN to the north-east world and caters to westbound flights entering SEAN from the north-east world.

The criticality of link “MABAL – VISAT” not only depends on its high traffic density and its presence on the major ATS route M758, but also depends on its position in the airspace. Link “MABAL – VISAT” is located in the busiest sector in the airspace covered by SEAN, with the highest traffic load and complexity. The trunk route M758 intersects with the major ATS routes M771 and N892, which cater for

**TABLE 2:** Characteristic information of critical links “MABAL – VISAT”, “KILOT – OTLON”, “KILOT – LIPRO” and “RAXIM – VMR”. The right-heading arrow “→” represents that the information is for flights transiting in the same direction as presented in the table header, e.g., from “MABAL” to “VISAT”, and vice versa. “Entry - Exit in SEAN” denotes the entry waypoint and exit waypoint in SEAN of flights transiting through the corresponding critical link, which are visualized with the corresponding flight path in Figs. 10 and 11.

	MABAL – VISAT	LIPRO – KILOT	KILOT – OTLON	RAXIM – VMR
<b>ATS route</b>	M758	M761	M761	M771
<b>Direction</b>	bidirectional	bidirectional	bidirectional	unidirectional
<b>Length (nm)</b>	41	32	21	47
<b>Flight ratio</b>	10.68%	5.68%	5.68%	5.69%
<b>Peak #aircraft/15mins</b>	6 ~ 7	4 ~ 5	4 ~ 5	4 ~ 5
<b>Mean speed (knots)→</b>	474.4	472.8	485.9	—————
<b>Speed range (knots)→</b>	246.2 ~ 615.6	322.3 ~ 644.6	315.4 ~ 630.7	—————
<b>Mean speed (knots)←</b>	446.6	445.8	451.4	442.3
<b>Speed range (knots)←</b>	273.6 ~ 615.6	322.3 ~ 644.6	315.3 ~ 630.7	282.9 ~ 565.7
<b>Entry – Exit in SEAN→</b>	OLKIT – SAROX, GULIB – SAROX OLKIT – IDSEL TEGID – SAROX TEGID – IDSEL GULIB – IDSEL	AGOBA – SAROX KAMIN – SAROX AGOBA – OTLON KAMIN – OTLON	AGOBA – SAROX KAMIN – SAROX AGOBA – OTLON KAMIN – OTLON	—————
<b>Entry – Exit in SEAN←</b>	KIMAT – OLKIT KIMAT – AKMON KIMAT – LAXOR IDSEL – OLKIT IDSEL – LAXOR IDSEL – AKMON KIMAT – TERIX VMR – AKMON KIMAT – SAROX KIMAT – LUSMO	KIMAT – AGOBA KIMAT – KAMIN OTLON – AGOBA OTLON – KAMIN OTLON – ARUPA	KIMAT – AGOBA KIMAT – KAMIN OTLON – AGOBA OTLON – KAMIN OTLON – ARUPA	VMR – DUDIS PARDI – DUDIS VTK – DUDIS PU – DUDIS VMR – AKMON

flights to and from the north (China, Vietnam, Thailand, etc.) [47], [53], at the waypoints “VISAT” and “MABAL” respectively. Therefore, managing the confluence of the ATS route M771 and N892 against the South China Sea air traffic flow on ATS routes M758 is a demanding task and puts pressure on link “MABAL – VISAT” due to the complexity exacerbated by the high density of crossing air traffic [54].

**2) Spatial criticality of link “LIPRO – KILOT” and “KILOT – OTLON”:** Airway links “LIPRO – KILOT” and “KILOT – OTLON” are on ATS route M761 (bidirectional airway). The two links handle 5.68% of flights in SEAN. Both of them have a short length, 32nm and 21nm respectively, and handle 4 ~ 5 flights per 15 minutes. The traffic density on the two links reaches a relatively high level, considering the short lengths of the two links, leading to a short space of time for reaction.

“LIPRO – KILOT” and “KILOT – OTLON” locate on M761, which is a trunk route for air traffic in east – west direction. Table 2 presents the Entry – Exit waypoints in SEAN of flights transiting through links “LIPRO – KILOT” and “KILOT – OTLON”. The right-heading arrow indicates that the flights are transiting in the westbound direction of “LIPRO – KILOT” and “KILOT – OTLON”, and vice versa. The corresponding flight paths connecting the listed Entry –

Exit pairs are highlighted by red dashes in Fig. 10 (for east-bound flights) and Fig. 11 (for westbound flights). It can be observed from Fig. 10 that eastbound flights transit through “OTLON – KILOT – LIPRO” on ATS route M761 and spread to ATS route M761, M646 and N875, which accommodates the major flows of air traffic between east Malaysia and Peninsular Malaysia, Brunei, Philippine, Indonesia, etc [53]. Similarly, from Fig. 11 we can see that westbound flights enter Singapore FIR through ATS routes M646 and N875. Flights then merge to ATS route M761 and fly to the west through links “LIPRO – KILOT – OTLON”.

Similar to link “MABAL – VISAT”, besides their high traffic density and crucial position, links “LIPRO – KILOT” and “KILOT – OTLON” are located within the highly utilized sector (the sector highlighted in purple in Fig. 8). Additionally, ATS route M761 crosses ATS route M771 and N892, which handle major traffic flows to and from the north in SEAN [47], [53], at waypoints “OTLON” and “KILOT” respectively. Traffic flow on ATS route M761 crosses north-eastbound traffic flow on ATS route N884 at waypoint “LIPRO”. The high density of crossing traffic and the short space of time for reaction due to the short lengths of the two links have increased the pressure on handling the high volume of air traffic on links “LIPRO – KILOT” and



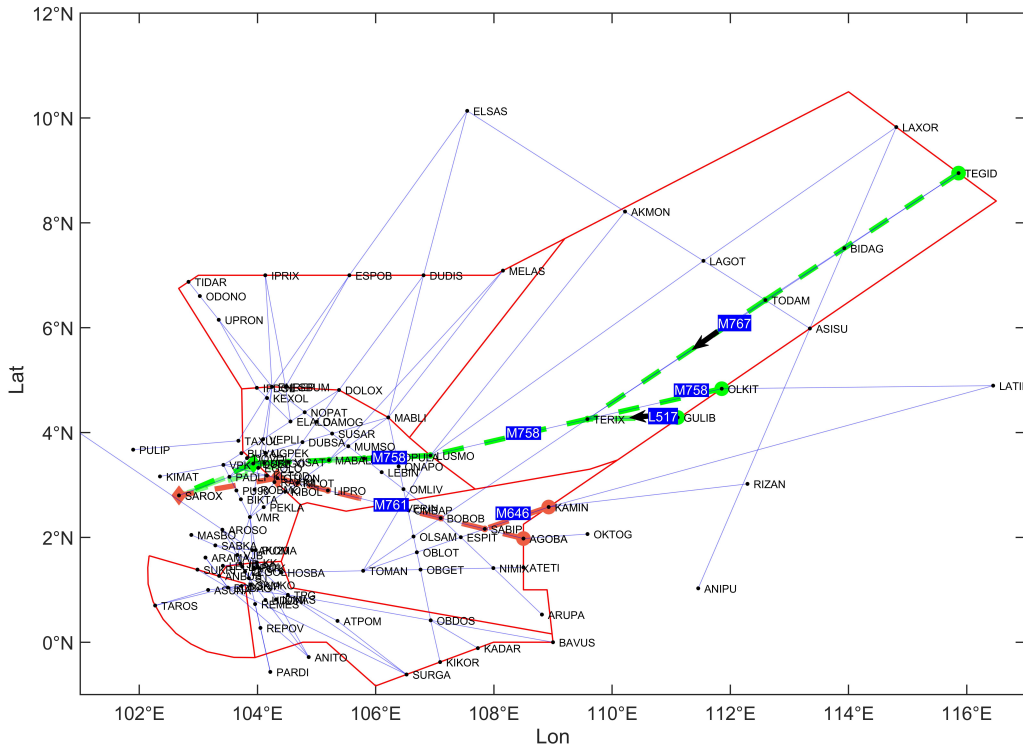


FIGURE 11: Routes of flights transiting through airway links identified through entry-exit waypoint as: “MABAL → VISAT” (green dashes), “LIPRO → KILOT → OTLON” (red dashes).

to descent as soon as possible. Considering the high traffic density and complexity on those links and the short time for reaction, the controllers must anticipate and solve such issues immediately.

**ii) Temporal view based on real-time traffic scenarios**

The above analyses manifest the criticality of the critical links from a spatial view. To manifest the efficacy of the critical link identification results from a temporal perspective, we have visualized the real-time flight movements with flight information (callsign, aircraft type, speed, flight level), as shown in Fig. 12. Two layers of flight traffic are shown in this figure as an example. Blue Dots represents aircraft in the airspace. The corresponding critical links identified under these traffic scenarios are marked in red and change dynamically over time.

This visualization will allow it to observe the traffic situations under different periods and validate the real-time critical link identification results dynamically. Here in this paper, two examples of air traffic scenarios and the corresponding critical links identified are shown.

As shown in Fig. 13a, at UTC time 01-Dec-2018 03:12:00, “MABAL – VISAT” (marked in red) is identified as a critical link. This time is 11:12:00 local time of Singapore. At this time, as shown in the figure, a high volume of flights transit through link “MABAL – VISAT” on ATS route M758, from both eastbound and westbound. Meanwhile, many north-east direction flights are flying along ATS route M771 and crossing traffic flow on M758 at waypoint “VISAT”. This situation leads to a potential area of conflict at “VISAT”. On

the rest of the network, either the traffic density is not high or the pressure of handling crossing traffic is low, making link “MABAL – VISAT” critical at this period.

As shown in Fig. 13b, “RAXIM – VMR” is identified as a critical link (marked in red) at UTC 01-Dec-2018 05:41:00. UTC 05:41 is between 13:00 and 14:00 local time of Singapore. At this time, more east-west bound flights are transiting through ATS routes M758 and M761, which can also be observed from Fig. 13b. Meanwhile, many flights transiting from Singapore to MERSING (“VMR”) are flying in north-north-east direction via ATS route M771. Traffic flow on M771 enters the sector filled with heavy traffic at waypoint “RAXIM”, which has a high density of flights at this time, and immediately crosses the east-west direction traffic flow on M761. This situation puts potential conflict pressure at “RAXIM”. Moreover, departure flights on “RAXIM – VMR” will need to step climb to the cruise level due to the crossing traffic on M761. This also adds to traffic complexity on the link “RAXIM – VMR”. The above facts make “RAXIM – VMR” a critical link at this moment compared to other links.

The above analyses from the perspective of traffic volumes, aeronautical charts, and the operational perspective manifest that the proposed method is effective in identifying critical airway links and can dynamically identify critical links over time in accordance with changing traffic conditions.

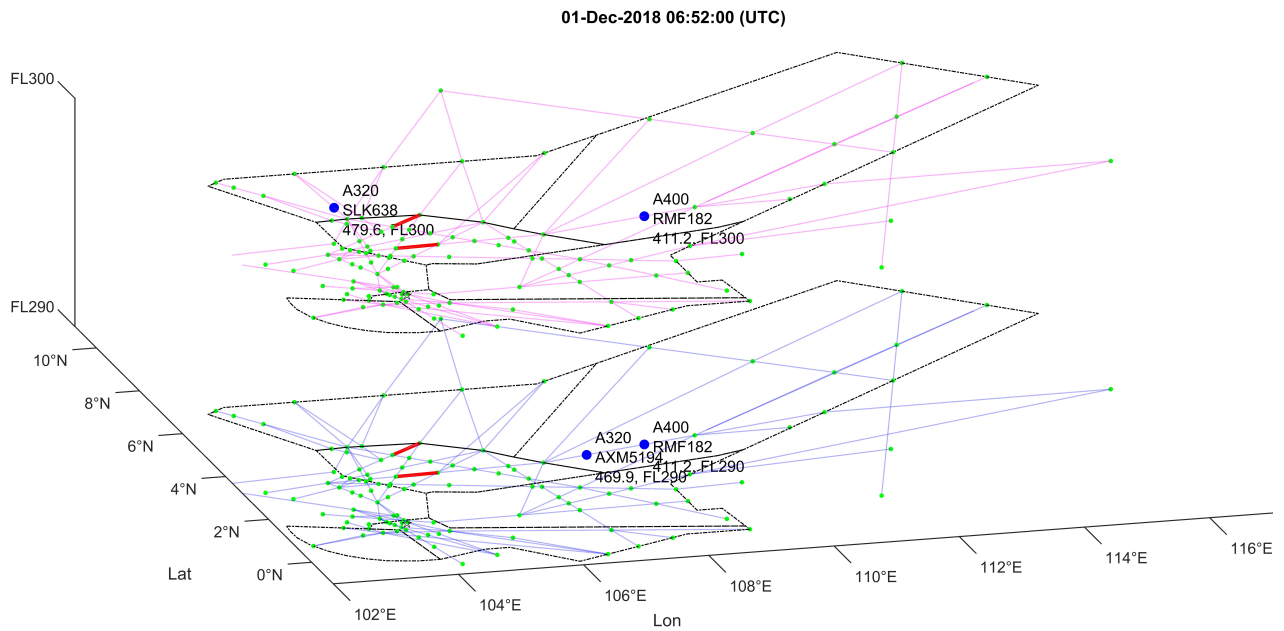


**FIGURE 12:** Real-time visualization and simulation of air traffic data for SMEs' analysis. The corresponding critical links identified under the traffic scenario are marked as red segments. Only two flight levels, out of eleven, and the corresponding air traffic is illustrated in this figure. The critical link identified evolves over time in accordance with the changes in air traffic.

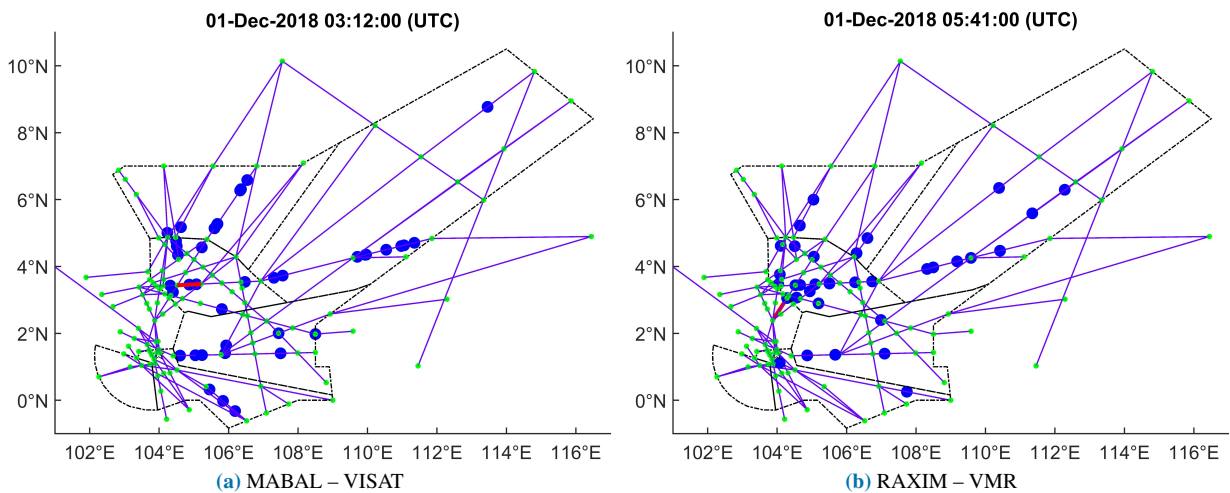


**FIGURE 13:** Examples of traffic scenarios under which “MABAL – VISAT” or “RAXIM – VMR” is identified as a critical link. The critical links are marked in red. Each blue dot represents one flight in SEAN.

## VI. CONCLUSIONS

Note that identifying critical links in an airway network can assist with air traffic flow management, flight scheduling, and resource allocation. This paper proposed complex network models to detect critical links in a given airway network dynamically. In order to quantify how critical a link of an airway network is, two metrics were introduced, i.e., edge betweenness centrality (identify links act as the traffic pivots with which shortest paths frequently pass through) and percolation theory (identify links that act as the bridges whose failures will decrease the network's structural integrity significantly). As the critical links of an airway network can vary over time, spatial-temporal airway networks were

constructed based on flight track data. Then the two network metrics were individually applied to each network snapshot for critical link detection, and their results were spatially intersected to determine the final critical links.

The proposed methodology is generic in the sense that it can be applied to any air traffic network given the sufficient data on air traffic. However, critical links detection in some air traffic networks might be challenging. For example, in European airspace, air traffic has significant vectoring, while in Chinese airspace, air traffic usually adheres to flight plans in en-route airspace. The proposed method was applied on SEAN with one-month flight track data. The detection results showed that the critical links in SEAN vary over time. The

majority of the links were concentrated in the sector that witnessed heavy transition traffic in the airspace covered by SEAN. Some of the critical links appeared with a high frequency and amongst which the four airway links “MABAL – VISAT”, “KILOT – OTLON”, “KILOT – LIPRO”, and “RAXIM – VMR” distinguished themselves from the rest.

Furthermore, we noticed that the four critical links belong to airways connecting two navigation aids (VOR/DME) or connecting one navigation aid (VOR/DME) to an important metering point. Observations from aeronautical charts showed that waypoints “MABAL”, “VISAT”, “OTLON”, “KILOT”, “LIPRO” and “RAXIM” are the crossing points of airways on the outbound radial of three navigation aids (PEKAN VOR/DME, KUCHING VOR/DME and MERSING VOR/DME), while the waypoint “VMR” is a metering fix. These observations manifest that the detected critical links based on the proposed method have operational significance. Further operational analysis by controllers validates the operational criticality of the detected critical links from both spatial and temporal views.

It is expected that the proposed method, which is based on complex network theory, can help identify dynamic airway links that are operationally critical as identified by SMEs. Moreover, considering the temporal nature of the proposed method, with good traffic flow prediction tools in the future, this method can be adopted to predict critical links in airway networks, which can help allocate resources in the airspace better and assist controllers in real-time air traffic management. Once a link is identified as critical for a given time period, ATFM measures can be applied in advance to prevent the potential failure of the critical link to reduce its impact on the flow of air traffic. On the strategic planning and pre-tactical planning stages of ATFM, by examining the forthcoming demand and assessing the traffic pressure on the critical links (such as the aforementioned four critical links), steps can be taken to balance the traffic pressure and operational efficiency on the critical links such as arranging with the Air Navigation Service Providers (ANSPs) to provide adequate capacity on the critical links at the required time, optimizing air traffic flows to reduce the traffic pressure on the critical links, scheduling or rescheduling flights as appropriate to avoid the critical links, and deciding the need for tactical ATFM measures on the critical links. On Tactical ATFM operations, re-routing traffic and flight level allocation can be applied according to the changing traffic situation and the corresponding critical links to ensure the smooth flow of air traffic through the air traffic network.

## REFERENCES

- [1] S. Gudmundsson, M. Cattaneo, and R. Redondi, “Forecasting temporal world recovery in air transport markets in the presence of large economic shocks: The case of covid-19,” *Journal of Air Transport Management*, vol. 91, p. 102007, 2021.
- [2] F. Netjasov, “Framework for airspace planning and design based on conflict risk assessment: Part 1: Conflict risk assessment model for airspace strategic planning,” *Transportation Research Part C: Emerging Technologies*, vol. 24, pp. 190–212, 2012.
- [3] D. Delahaye and S. Puechmorel, “Air traffic complexity based on dynamical systems,” in *49th IEEE Conference on Decision and Control (CDC)*, Atlanta, GA, USA. IEEE, 15-17 December, 2010, pp. 2069–2074.
- [4] M. Bagamanova and M. M. Mota, “A multi-objective optimization with a delay-aware component for airport stand allocation,” *Journal of Air Transport Management*, vol. 83, p. 101757, 2020.
- [5] IATA, “European air traffic control delays loom over summer air travel,” <https://www.iata.org/pressroom/pr/Pages/2018-07-18-01.aspx>, 2018, accessed on January 28, 2019.
- [6] W. Du, M. Zhang, Y. Zhang, X. Cao, and J. Zhang, “Delay causality network in air transport systems,” *Transportation Research Part E: Logistics and Transportation Review*, vol. 118, pp. 466–476, 2018.
- [7] X. Sun and S. Wandelt, “Network similarity analysis of air navigation route systems,” *Transportation Research Part E: Logistics and Transportation Review*, vol. 70, pp. 416–434, 2014.
- [8] A. Wellens and M. M. Mota, “Modeling approach for managing the demand in congested airport networks: The case of mexico city airport,” in *2017 Winter Simulation Conference (WSC)*. IEEE, 2017, pp. 4535–4537.
- [9] D. Chen, M. Hu, H. Zhang, J. Yin, and K. Han, “A network based dynamic air traffic flow model for en route airspace system traffic flow optimization,” *Transportation Research Part E: Logistics and Transportation Review*, vol. 106, pp. 1–19, 2017.
- [10] C. Hurter, Y. Brenier, J. Ducas, and E. Le Guilcher, “Cap: Collaborative advanced planning, trade-off between airspace management and optimized flight performance: Demonstration of en-route reduced airspace congestion through collaborative flight planning,” in *2016 IEEE/AIAA 35th Digital Avionics Systems Conference (DASC)*, Sacramento, CA, USA. IEEE, 25-29 Sept. 2016, pp. 1–9.
- [11] C. Chen and W. Du, “A multi-objective crossing waypoints location optimization in air route network,” in *2011 3rd International Workshop on Intelligent Systems and Applications*, Wuhan, China. IEEE, 28-29 May 2011, pp. 1–4.
- [12] W. Shijin, C. Xi, L. Haiyun, L. Qingyun, H. Xu, and W. Yanjun, “Air route network optimization in fragmented airspace based on cellular automata,” *Chinese Journal of Aeronautics*, vol. 30, no. 3, pp. 1184–1195, 2017.
- [13] C. Ma, Q. Cai, S. Alam, B. Sridhar, and V. N. Duong, “Airway network management using braess’s paradox,” *Transportation Research Part C: Emerging Technologies*, vol. 105, pp. 565–579, 2019.
- [14] D. Li, B. Fu, Y. Wang, G. Lu, Y. Berezin, H. E. Stanley, and S. Havlin, “Percolation transition in dynamical traffic network with evolving critical bottlenecks,” *Proceedings of the National Academy of Sciences*, vol. 112, no. 3, pp. 669–672, 2015.
- [15] A. Cook, H. A. Blom, F. Lillo, R. N. Mantegna, S. Micciche, D. Rivas, R. Vázquez, and M. Zanin, “Applying complexity science to air traffic management,” *Journal of Air Transport Management*, vol. 42, pp. 149–158, 2015.
- [16] E. Yu, D. Chen, and J. Zhao, “Identifying critical edges in complex networks,” *Scientific Reports*, vol. 8, no. 1, pp. 1–8, 2018.
- [17] L. Liu, B. Yin, S. Zhang, X. Cao, and Y. Cheng, “Deep learning meets wireless network optimization: Identify critical links,” *IEEE Transactions on Network Science and Engineering*, vol. 7, no. 1, pp. 167–180, 2018.
- [18] Q. Cai, M. Pratama, and S. Alam, “Interdependency and vulnerability of multipartite networks under target node attacks,” *Complexity*, vol. 2019, Art. No. 2680972, 2019.
- [19] D. Z. Wang, H. Liu, W. Szeto, and A. H. Chow, “Identification of critical combination of vulnerable links in transportation networks—a global optimisation approach,” *Transportmetrica A: Transport Science*, vol. 12, no. 4, pp. 346–365, 2016.
- [20] X. Xu, A. Chen, and C. Yang, “An optimization approach for deriving upper and lower bounds of transportation network vulnerability under simultaneous disruptions of multiple links,” *Transportation Research*, vol. 94, no. 9, pp. 338–353, 2018.
- [21] E. L. de Oliveira, L. da Silva Portugal, and W. P. Junior, “Indicators of reliability and vulnerability: Similarities and differences in ranking links of a complex road system,” *Transportation Research Part A: Policy and Practice*, vol. 88, pp. 195–208, 2016.
- [22] P. Gauthier, A. Furno, and N.-E. El Faouzi, “Road network resilience: how to identify critical links subject to day-to-day disruptions,” *Transportation Research Record*, vol. 2672, no. 1, pp. 54–65, 2018.
- [23] R. Vodák, M. Bíl, T. Svoboda, Z. Křivánková, J. Kubeček, T. Rebok, and P. Hliněný, “A deterministic approach for rapid identification of the critical links in networks,” *PloS One*, vol. 14, no. 7, p. e0219658, 2019.
- [24] M. Du, X. Jiang, and L. Cheng, “Alternative network robustness measure using system-wide transportation capacity for identifying critical links in

- road networks,” *Advances in Mechanical Engineering*, vol. 9, no. 4, pp. 1–12, 2017.
- [25] M. Guettiche and H. Kheddouci, “Critical links detection in stochastic networks: application to the transport networks,” *International Journal of Intelligent Computing and Cybernetics*, vol. 12, no. 1, pp. 42–69, 2019.
- [26] P. Ren and L. Li, “Characterizing air traffic networks via large-scale aircraft tracking data: A comparison between china and the us networks,” *Journal of Air Transport Management*, vol. 67, pp. 181–196, 2018.
- [27] T. Bröhl and K. Lehnertz, “Centrality-based identification of important edges in complex networks,” *Chaos: An Interdisciplinary Journal of Non-linear Science*, vol. 29, no. 3, p. 033115, 2019.
- [28] I. Kivimäki, B. Lebichot, J. Saramäki, and M. Saerens, “Two betweenness centrality measures based on randomized shortest paths,” *Scientific Reports*, vol. 6, no. 1, pp. 1–15, 2016.
- [29] Y. Shen, N. P. Nguyen, Y. Xuan, and M. T. Thai, “On the discovery of critical links and nodes for assessing network vulnerability,” *IEEE/ACM Transactions on Networking*, vol. 21, no. 3, pp. 963–973, 2012.
- [30] E. L. de Oliveira, L. da Silva Portugal, and W. P. Junior, “Determining critical links in a road network: vulnerability and congestion indicators,” *Procedia-Social and Behavioral Sciences*, vol. 162, pp. 158–167, 2014.
- [31] C. Yang, A. Chen, X. Xu, and S. Wong, “Sensitivity-based uncertainty analysis of a combined travel demand model,” *Transportation Research Part B: Methodological*, vol. 57, pp. 225–244, 2013.
- [32] H. Feng, F. Bai, and Y. Xu, “Identification of critical roads in urban transportation network based on GPS trajectory data,” *Physica A: Statistical Mechanics and its Applications*, vol. 535, p. 122337, 2019.
- [33] X. Yang, L. Liu, Y. Li, and R. He, “Identifying critical links in urban traffic networks: a partial network scan algorithm,” *Kybernetes*, vol. 45, no. 6, pp. 915–930, 2016.
- [34] Y. Zhou and J. Wang, “Critical link analysis for urban transportation systems,” *IEEE Transactions on Intelligent Transportation Systems*, vol. 19, no. 2, pp. 402–415, 2017.
- [35] T. Bröhl and K. Lehnertz, “Centrality-based identification of important edges in complex networks,” *Chaos: An Interdisciplinary Journal of Non-linear Science*, vol. 29, no. 3, p. 033115, 2019.
- [36] F. Morone and H. A. Makse, “Influence maximization in complex networks through optimal percolation,” *Nature*, vol. 524, no. 7563, pp. 65–68, 2015.
- [37] S. Boccaletti, J. Almindral, S. Guan, I. Leyva, Z. Liu, I. Sendiña-Nadal, Z. Wang, and Y. Zou, “Explosive transitions in complex networks’ structure and dynamics: Percolation and synchronization,” *Physics Reports*, vol. 660, pp. 1–94, 2016.
- [38] Q. Cai, M. Pratama, S. Alam, C. Ma, and J. Liu, “Breakup of directed multipartite networks,” *IEEE Transactions on Network Science and Engineering*, vol. 7, no. 3, pp. 947–960, 2019.
- [39] P. Baumgarten, R. Malina, and A. Lange, “The impact of hubbing concentration on flight delays within airline networks: An empirical analysis of the us domestic market,” *Transportation Research Part E: Logistics and Transportation Review*, vol. 66, pp. 103–114, 2014.
- [40] ICAO, ICAO PANS-ATM Doc.4444, ATM/501, 15th Edition, Procedures for Air Navigation Services. ICAO, 2010.
- [41] M. Barthélemy, “Spatial networks,” *Physics Reports*, vol. 499, no. 1-3, pp. 1–101, 2011.
- [42] T. Lehouillier, F. Soumis, J. Omer, and C. Allignol, “Measuring the interactions between air traffic control and flow management using a simulation-based framework,” *Computers & Industrial Engineering*, vol. 99, pp. 269–279, 2016.
- [43] C. Verlhac and S. Manchon, “Optimization of opening schemes,” in Proceedings of the fourth USA/Europe Air Traffic Management R&D Seminar, Santa, USA, 4-7 Dec. 2001, pp. 8–49.
- [44] K. Pien, K. Han, W. Shang, A. Majumdar, and W. Ochieng, “Robustness analysis of the european air traffic network,” *Transportmetrica A: Transport Science*, vol. 11, no. 9, pp. 772–792, 2015.
- [45] S. Starita, A. K. Strauss, X. Fei, R. Jovanović, N. Ivanov, G. Pavlović, and F. Fichert, “Air traffic control capacity planning under demand and capacity provision uncertainty,” *Transportation Science*, vol. 54, no. 4, pp. 882–896, 2020.
- [46] K. Hanson, J. Gulding, and A. Afshar, “Analyzing the operational capacity effects of the monitor alert paramater (MAP),” in 2016 Integrated Communications Navigation and Surveillance (ICNS), Herndon, VA, USA. IEEE, 19-21 April 2016, pp. 6C1–1.
- [47] ICAO, “Report of the fourth meeting of the southeast Asia route review task force,” [https://www.icao.int/APAC/Meetings/2010/sea\\_rr\\_tf4/SEA-RRTF4rpt.pdf](https://www.icao.int/APAC/Meetings/2010/sea_rr_tf4/SEA-RRTF4rpt.pdf), 2010, accessed on March 18, 2021.
- [48] J. Milan, “A practical capacity model of an air route network,” *Transportation Planning and Technology*, vol. 11, no. 2, pp. 87–103, 1986.
- [49] X. Sun, S. Wandelt, and F. Linke, “On the topology of air navigation route systems,” in Proceedings of the Institution of Civil Engineers-Transport, vol. 170, no. 1. Thomas Telford Ltd, 2017, pp. 46–59.
- [50] A. Winick and D. Brandewie, “VOR/DME system improvements,” *Proceedings of the IEEE*, vol. 58, no. 3, pp. 430–437, 1970.
- [51] “Aeronautical information publication & amendments,” <https://www.caas.gov.sg/docs/default-source/pdf/aip-singapore—31-dec-20.pdf>, 2020, accessed on February 8, 2021.
- [52] SkyVector, “SkyVector aeronautical charts,” <https://skyvector.com>, 2021, accessed on March 30, 2021.
- [53] ICAO, “The fourth meeting of traffic flow review group: Harmonisation of effort to restructure ATS routes over the South China Sea,” <https://www.icao.int/APAC/Meetings/2016%20SCSTFRG4/SCSTFRG4%20WP06%20Harmonization%20of%20Effort%20to%20Restructure%20ATS%20Routes%20Over%20the%20South%20China%20Sea-Singapore.pdf>, 2016, accessed on March 18, 2021.
- [54] —, “The fourth meeting of South China Sea traffic flow review group: Harmonization of parallel routes structure with existing ATS routes M751 within Kuala Lumpur FIR and M644 within Bangkok FIR,” <https://www.icao.int/APAC/Meetings/2016%20SCSTFRG4/SCSTFRG4%20WP13%20Harmonization%20of%20Parallel%20Routes%20Structure%20with%20Existing%20ATS%20Routes%20M751%20within%20KUALA%20LUMPUR%20FIR%20and%20M644.pdf>, 2016, accessed on March 18, 2021.



**CHUNYAO MA** is a PhD student at the Air Traffic Management Research Institute, Nanyang Technological University, Singapore. She obtained her M.S. degree in aerospace engineering from Nanjing University of Aeronautics and Astronautics. Her research interests include big data analytics and artificial intelligence with wide applications to solving air traffic flow management and airspace design issues.



**QING CAI** received the B.S. degree in electronic information engineering from Wuhan Textile University, Wuhan, China, in 2010. He received the Ph.D. degree in Pattern Recognition and Intelligent Systems at the School of Electronic Engineering, Xidian University, Xi'an, China, in 2015. His current research interests are in the area of artificial intelligence, complex network analytics, recommender systems, air traffic management and bioinformatics.



**SAMEER ALAM** received the M.S. degree in computer science from Birla Institute of Technology, Mesra, India, in 1999 and the Ph.D. degree in computer science from University of New South Wales, Canberra, Australia, in 2008. He is currently an Associate Professor with the School of Mechanical and Aerospace Engineering, Nanyang Technological University. His research interests include simulation, modelling, risk assessment, and the optimization of advanced air traffic management concepts. Dr. Alam is the Founding Member of the IEEE Computational Intelligence Society Chapter in Canberra. He is a Chief Investigator of ICAOMIDRMA Collision Risk Project and served as a Co-Chief Investigator for several projects of Air Service Australia and EUROCONTROL. He is a recipient of the Australian National University Science Medal in 2011, the Tall Poppy Science Award in 2011, and the Fresh Science Award in 2009.



**DANIEL DELAHAYE** is the head of the Optimization and Machine Learning Team of the ENAC research laboratory (ENAC : French Civil Aviation University). He is also in charge of the research chair "AI for ATM and Large Scale Urban Mobility" in the new AI institute ANITI in Toulouse. He obtained his engineer degree from the ENAC school and did a Masters of Science in Signal Processing from the National Polytechnic Institute of Toulouse in 1991. He graduated with a

PH.D in automatic control from the Aeronautic and Space National School in 1995 under the co-supervision of Marc Schoenauer (CMAPX) and did a post-doc at the Department of Aeronautics and Astronautics at MIT in 1996 under the supervision of Professor Amedeo Odoni. He conducts research on mathematical optimization and artificial intelligence for airspace design and aircraft trajectories optimization. He actively collaborates with MIT, Georgia Tech and NASA (USA) on development of Artificial Intelligence algorithms for air traffic management applications.

• • •